



Conditional Loss-of-Growth 1 (CLog1) is a Novel Protein that Localizes to Microtubules in *Physcomitrella patens*

By

Sakshi Khurana

Submitted to the Department of Biology and Biotechnology in partial fulfillment of the requirements for the degree of

Bachelor of Science

at

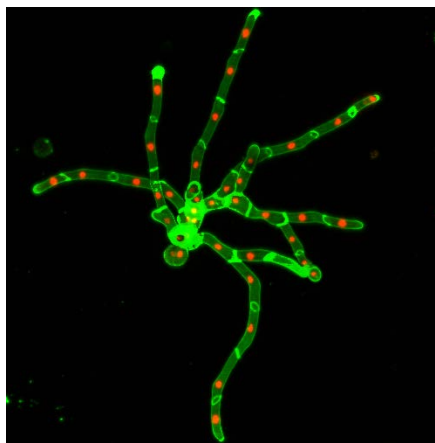
WORCESTER POLYTECHNIC INSTITUTE

April 28, 2016

© Sakshi Khurana, MMXVI. All rights reserved.

Certified by Luis Vidali

Associate Professor, Department of Biology & Biotechnology



This report represents the work of a WPI undergraduate student submitted to the faculty as evidence of completion of a degree requirement. WPI routinely publishes these reports on its website without editorial or peer review. For more information about the projects program at WPI, please see <http://www.wpi.edu/academics/ugradstudies/project-learning.html>

Abstract

Understanding the genetic basis of plant cell development is important for future agricultural improvements, especially with the increase in global food demand. In this study, the intracellular localization of CLoG1 was used to investigate the function of this novel gene. CLoG1 was previously identified by screening temperature sensitive (TS) mutants with impaired growth at the restrictive temperature; this type of screen is simplified in the moss *Physcomitrella patens* because of its predominant haploid state. Initially, the functionality of green fluorescent protein (mEGFP) tagged CLoG1 was demonstrated using a transient complementation assay. In this assay, plants with silenced CLoG1 were co-transformed with CLoG1:mEGFP N or C-terminal fusions, and growth was analyzed. Once it was established that the fusions were functional, stable cell lines of *P. patens* were generated expressing the CLoG1:mEGFP constructs. Using laser scanning confocal microscopy, the apical cells in protonemal filaments were imaged, which revealed an association with the microtubule cytoskeleton. CLoG1:mEGFP fusions were found to associate with the mitotic spindle and phragmoplast, suggesting a role in cell division. To investigate the participation of CLoG1 in cell division, CLoG1 TS mutants transformed with a nuclearly localized GFP construct were analyzed at permissive and restrictive temperatures. This allowed evaluation of the impact of the CLoG1 mutation on cell numbers and nuclear division. Though we did not find evidence of multinucleated cells, the mutation causes a decrease in the size and number of cells. This study provides insights into the function of the CLoG1 protein and its role in plant cell growth.

Acknowledgements

I would like to thank Victoria Huntress for her assistance with the microscopy in this study and the members of the Bezanilla and Vidali lab for their continued support and guidance. I would also like to thank the NSF for summer work support under the grant NSF:MCB:1253444 to L.V.

Table of Contents

Abstract.....	i
Acknowledgements	ii
Table of Contents	iii
List of Figures	iv
List of Tables	iv
Background.....	1
Importance of Plant Development and Morphogenesis.....	1
Factors in Plant Growth.....	3
Advantages of <i>Physcomitrella patens</i> as a Model Organism.....	5
Importance of Conditional Mutants	7
Previous Work	8
Identifying Localization and Function.....	11
Project Objectives	13
Methods and Materials	15
Moss Culture and Protoplasting	15
Transformations	15
CLOG1:mEGFP Fusion Construction.....	16
RNAi Complementation Assay	18
Localization	19
Nuclear Counting Assay	20
Results.....	21
Restriction Analysis of CLOG1:mEGFP Fusions.....	21
RNAi Complementation Assay	22
Localization	24
Nuclear Counting Assay	27
Discussion	30
Fusion Constructs.....	30
RNAi Complementation Assays	31

Localization	31
Nuclear Counting Assay	32
Future Experiments.....	33
References	35
Appendices	39
APPENDIX I: Moss medium recipes	39
APPENDIX II: ImageJ macro for area and solidity quantification created by Jeffrey Bibeau, a member of the Vidali Lab	40
APPENDIX III: ImageJ macro for nuclear counting.....	58

List of Figures

Figure 1. Total project world population in thousands.....	1
Figure 2. Phylogenetic tree of CLoG1	10
Figure 3. Restriction analysis.....	22
Figure 4. RNAi complementation assay images.....	23
Figure 5. Normalized area and solidity of RNAi complementation assay.....	24
Figure 6. Confocal microscopy of tip growing cell.	25
Figure 7. Confocal microscopy of dividing cell.	26
Figure 8. Nuclear counting assat representative plants	28
Figure 9. Average number of nuclei per plant.....	29

List of Tables

Table 1. Expected fragment lengths.....	21
--	----

Background

Importance of Plant Development and Morphogenesis

The importance of understanding plant growth and morphogenesis has never been so crucial. With the United Nations projecting a world population of 8.14 billion people 2025 as shown in Figure 1, ensuring sufficient food production and distribution is vital. Furthermore, the United Nations World Food Programme (WFP) estimates that approximately 795 million people in the world do not have enough food to lead a healthy active life, which is equivalent to one in nine people (FAO, 2015).

Notwithstanding economic distribution problems, increasing crop yields is a viable solution to the growing concern of world hunger and agricultural biotechnology holds the answers to increasing the nutritional content of our crops.

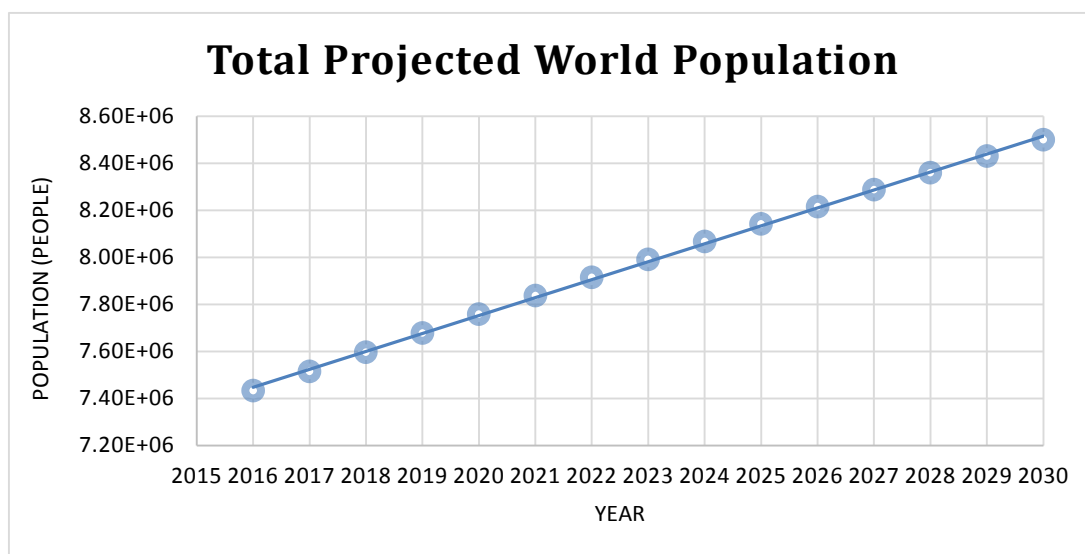


Figure 1. Total project world population in thousands. Data acquired from United Nations, Department of Economic and Social Affairs, Population Division (2015)

Much effort has been put into using plant biotechnology to solve the increasing global food problems, namely the Green Revolution between 1930 and 1960. Led by Norman Borlaug, an American plant biologist, the series of research and development initiatives resulted in increased agricultural production around the world mostly due to the development of high yield cereals, synthetic fertilizer and pesticides. Despite the drawbacks of the revolution such as the impact of chemicals on biodiversity, it played a significant role in raising awareness and recognition of the benefits of plant biotechnology in improving the quality of life experience for humans (Borlaug, 2000).

However successful past actions have been, more must be done to support the expanding population. As more scientists focus on agricultural and plant biotechnology, it is first important to understand the fundamentals of plant development and morphogenesis. The growth of plants is a common theme in genetic engineering experiments. For example, many agricultural scientists are modifying crops to survive better in certain conditions. In 2001, the University of Toronto explored transgenic tomato plants that overexpressed a Na^+/H^+ antiporter. These plants were able to grow, flower and produce fruits in high salt concentrations while the wild type exhibited stunted growth. The plants accumulate high salt content in their leaves but not their fruits, suggesting that a transgenic system such as this one can be used viably for agricultural purposes (Zhang and Blumwald, 2001).

Plant development is also important for studies attempting to increase biofuel production. There is a need for bioenergy as a viable alternative to traditional

petroleum-based fuel in order to reduce carbon dioxide emission and improve environmental and economic sustainability. There are several biotechnological methods to modify plant growth and development for use in biofuel production. Explored processes include lignin biosynthesis modification, cellulase expression, abiotic stress resistance and increasing biomass. Understanding the pathways that control growth is important because, for example, dwarfing a plant could produce lower lignin, increase cellulosic content and result in a shift of biomass to the leaves (Yuan et al., 2008). Evidently, investigating the genetic basis of plant cell growth and development are critical to solve agricultural and biofuel production problems.

Factors in Plant Growth

There are many factors that help regulate cell shape and growth. Plant cells are eukaryotic cells but they differ from animal cells in that they have a cell wall and are largely composed of vacuoles. However, just like animal cells, plant cells possess a cytoskeleton. The cytoskeleton is a collection of network filaments that extends throughout the cytoplasm of the cell and is generally comprised of three types of filaments: actin filaments, microtubules and intermediate filaments. Though intermediate filaments have not been identified in plants, much research exists on actin and microtubules in plant cells. In addition to filaments, there are motor proteins such as myosin, kinesins and dyneins that move along these filaments in an energy dependent manner to transport molecules or organelles (Kost and Chua, 2002).

Plant cell growth is driven by turgor pressure. However, there are mechanisms in place to help control the growth. During diffuse growth, cortical microtubules are usually aligned in a transverse orientation, perpendicular to the main axis of cell growth. They play an important role in the deposition of cellulose microfibrils which control cell expansion as a part of the cell wall (Kost and Chua, 2002). Mutations that disrupt the microtubules cause aberrant orientation of the cellulose microfibrils and reduce cell elongation (Burk and Ye, 2002). The current working model of the microtubule-cellulose relationship is an enzyme complex, which uses microtubules as a guide for synthesizing and depositing cellulose microfibrils in the cell wall. Thus, microtubules help prevent radial growth and influence the direction of cell elongation. During cell division, microtubules reorganize into the mitotic spindle and later develop into the phragmoplast, a structure involved in cell wall construction between the two new cells during cytokinesis. Motor proteins such as kinesins are responsible for transporting Golgi-derived secretory vesicles along the phragmoplast microtubules to the growing cell plate (Kost and Chua, 2002). During tip growth however, microtubules become longitudinally oriented and are involved with directionality control by stabilizing a single point of growth (Hepler et al., 2001).

The other significant type of filament important for tip growing plant cells is actin. Actin networks are highly dynamic. They form long cables that are longitudinally oriented along the length of tip growing cells along with a dense network of filaments near the tip. The function of actin was elucidated through experiments using actin

depolymerization drugs such as cytochalasins and latrunculins, which cause an arrest in growth (Vidali et al., 2001). Actin is involved with the movement of vesicles across the cells, which ferry materials needed for growth to the tip of the cells. This process, similar to that of kinesins, requires the motor protein myosin, which drives Golgi-derived vesicles along the length of actin filaments using cytoplasmic streaming (Kost and Chua, 2002). Together, microtubules and actin filaments interact to form a complex that is required for tip growth. The microtubules are thought to organize actin filaments into bundles that allow for cytoplasmic streaming (Hepler et al., 2001).

It is also important to mention another aspect of plant growth: plant growth regulators (PGRs). Also called plant hormones, these compounds have varying effects on gene expression, transcription and cell division. There are five common groups of PGRs: auxins, cytokinins, gibberellins, ABA and ethylene (Nemhauser et al., 2006) but there is no evidence that they are directly implicated in tip growth.

Advantages of *Physcomitrella patens* as a Model Organism

Physcomitrella patens is a moss that is commonly used in genetic studies (Nishiyama et al., 2003). The moss is a bryophyte, a non-vascular land plant which reproduces through spores. The haploid spore germinates to form protonema, a filamentous network of cells. The protonemal filaments grow by polarized growth with the stem cell at the apex of the filaments. The polarized growth of *P. patens* protonema is particularly useful for microscopy because single, actively growing cells can be easily visualized. The apical cells differentiate into two types of cells: chloronema and

caulonema. Chloronema are chloroplast-rich cells with transverse cell walls. Caulonema cells are fast growing, contain less chloroplasts and have cell walls oblique to the long axis of the cell. The simple morphology of these protonemal filaments allows for visualization of developmental phenotypes (Prigge and Bezanilla, 2010).

In addition to the morphological benefits, *P. patens* has a predominantly haploid life cycle (Cove et al., 2009). The haploid nature of the genome allows for efficient gene targeting. Homologous recombination allows for DNA integration at high frequencies (Schaefer and Zryd, 1997). In experiments targeting three single-copy loci, a team of Swiss scientists reported a targeting efficiency of 90% which is higher than ever recorded for gene targeting in plants. This level of efficiency has only been previously observed in low order eukaryotes such as yeast, fungi and protozoa (Schaefer and Zryd, 1997). With the ability to perform efficient gene targeting along with the availability of the complete genome sequence, *P. patens* is an ideal model system for reverse genetic studies. RNA interference (RNAi) can be used to knock down specific genes and observe the phenotypic effects and thus, analyze gene function (Bezanilla et al., 2005).

The ease of culturing *P. patens* is another valuable property of the moss. The moss allows for vegetative propagation. The cells can be mechanically disrupted at any stage of development and the disrupted cells will convert back into chloronemal apical cells and continue their production of the filamentous network. This is the primary reason why mutant lines containing developmental weaknesses can be maintained. Furthermore, *P. patens* allows for protoplast generation. Protoplasts are single-celled

plants in an osmotically controlled solution that have been stripped of their cell wall by a digestive enzyme. Protoplasting has allowed for effective transfection and stable line production of *P. patens*. The transformation process, mediated by polyethylene glycol (PEG) can provide up to 7000 transient transformants or 200 stable transformants from 60 µg of DNA (Liu and Vidali, 2011).

Importance of Conditional Mutants

A significant problem in studying a mutation is lethality. If a mutation is lethal to the organism, a strain or cell line cannot be sustained. However, if the mutation is not lethal but causes a growth or fertility phenotype, the cell line might still be difficult to maintain. The simple solution to this problem is the development of conditional mutants. These conditional mutations allows the organism to resemble the wild type strain at certain conditions and display a characteristic phenotype at others (Pringle, 1975). Conditional mutants have previously been used in yeast studies extensively to understand gene function and identify molecular pathways (Hartwell, 1967).

A common type of conditional mutation used for plant genetics is temperature sensitivity, which has been used in past studies to investigate genes important for growth and morphology (Hartwell, 1967). Temperature sensitive mutants are characterized by their ability to grow at permissive temperatures while exhibiting stunted growth at restrictive temperatures. Here, the mutant phenotype is expressed in a line of *P. patens* which grows normally at 25°C and abnormally at 32°C. Allowing protoplasts to regenerate at the permissive temperature before assaying them at the

restrictive temperature, allows for the observation of the growth phenotype without causing death of the plants.

Previous Work

The focus of this study is the gene Conditional Loss-of-Growth 1 (*CLoG1*) which was identified and mapped in the *P. patens* genome in two previous Major Qualifying Projects by Xinxin Ding '14 (Ding, 2014) and Leah Pervere '15 (Pervere, 2015). In her work, Ding generated mutants using UV mutagenesis of the *P. patens* Gransden wild type strain. Protoplasts were treated with 1,100 J/m² of UV light and after four days of regeneration, plants smaller than 400µm were selected. The resulting mutants were proliferated at permissive and restrictive temperatures to test for temperature sensitivity. Ding isolated eight mutants and characterized their morphology and growth. In order to find the causal mutation against the background mutations induced by the UV mutagenesis, Ding took advantage of the properties of the Gransden and the polymorphic Villersexel strains of *P. patens*. Gransden displays low self-fertilization rates compared to outcrossing rates with Villersexel. The eight isolated mutants were outcrossed with a mCherry tagged Villersexel line, from which six outcrossed successfully (Ding, 2014).

For one of the mutants, *CLoG1*, 24 F1 segregants displaying the TS phenotype previously characterized were selected as the mapping population. DNA was extracted from the segregants, pooled, and the genomes were sequenced. The sequences were used to map the gene based on the principles of meiotic homologous recombination.

Spores have a 50% chance of inheriting a nucleotide from the one parent and 50% chance of inheriting a nucleotide from the other parent at any given location in their genome. Thus, the F1 progeny have 50% chance of resembling the Gransden strain and 50% of resembling Villersexel strain at any given nucleotide. This 50/50 ratio should be consistent throughout their genome with the exception of the region containing the causal mutation which should conserve the Gransden sequence (Ding, 2014). Thus, based on this principle, Ding was able to map the causal point mutation to position 4,325,703 on chromosome 24 where a guanine was substituted with an adenine (Pervere, 2015).

To confirm this location, Pervere conducted a rescue experiment. In this experiment, PCR was used to amplify and isolate the region from the wild type sequence that contains the mapped position. The PCR products were then transformed into TS mutant CLoG1 protoplasts. DNA was extracted from the transformed plants and PCR was conducted to isolate the region and then sequence it. Pervere was able to achieve rescuing in one transformed plant, evident by the adenine to guanine substitution at position 4,325,703 of chromosome 24 for that rescued plant (Pervere, 2015).

The identification of this causal mutation is important due to the relevance of CLoG1 for other species. Figure 2 shows a phylogenetic tree of CLoG1's homologous proteins. It is conserved in protists, green algae and all land plants. Understanding the protein's function in plant growth can truly impact crop production.

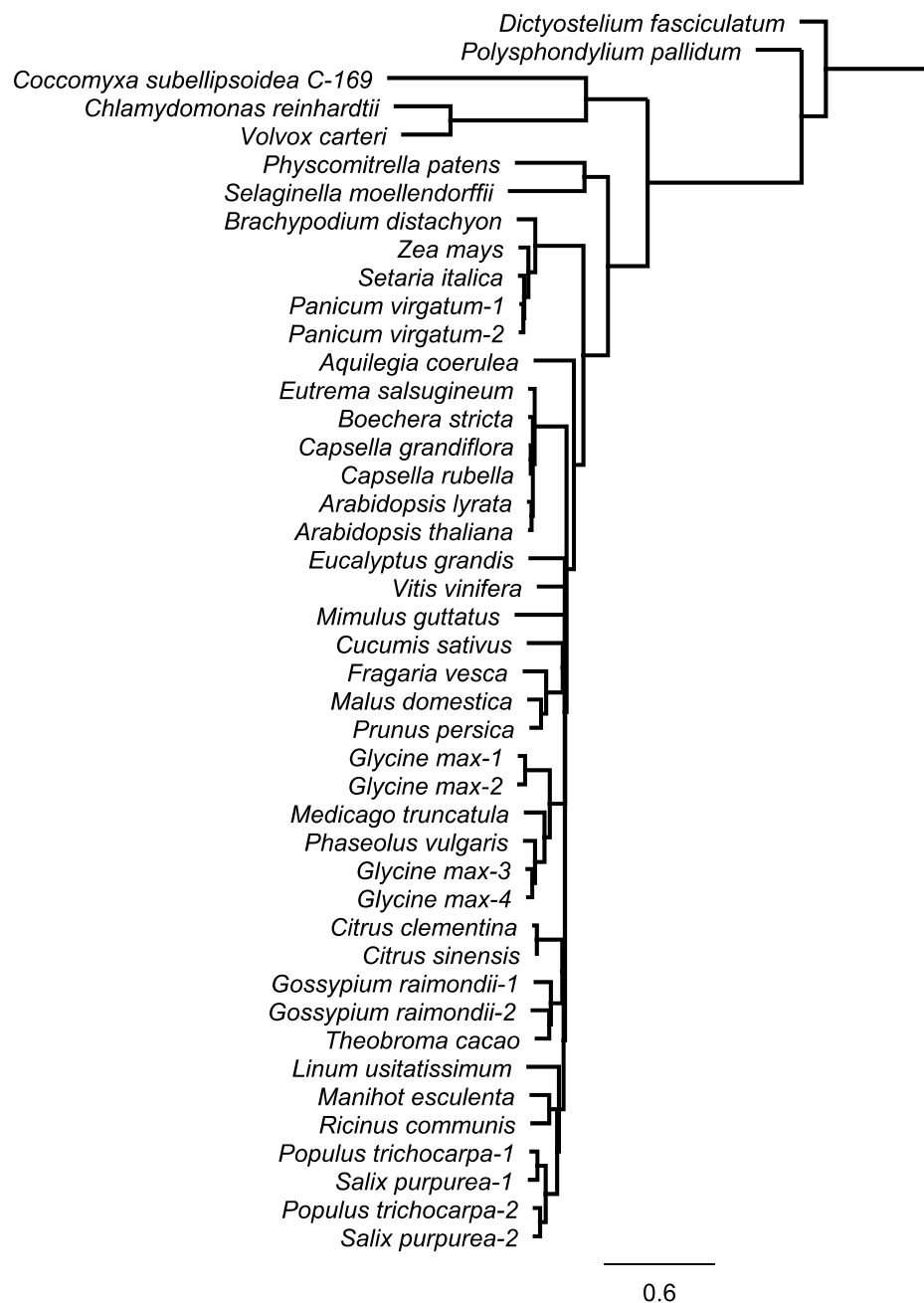


Figure 2. Phylogenetic tree of CLoG1 and homologous proteins shows conservation in all land plants indicating the importance of understanding protein function

Identifying Localization and Function

There are two general approaches to genetic studies. The most direct way is reverse genetics in which the phenotypic impact of removing or mutating a known gene on an organism is studied. Gene knockouts, targeted mutations, and RNA interference are common methods used in reverse genetics. The more classical approach is forward genetics in which random mutations are induced and a genetic screen is used to isolate mutants. The responsible genes for the observable phenotype can be identified along with its function (Alberts, 2002). This was the approach used for CLoG1 by Ding and Pervere (Ding, 2014; Pervere, 2015). With the phenotype of the CLoG1 mutants characterized and the gene identified, the next step is to investigate function.

There are several strategies to identify the function of novel genes and the proteins they code for. The first step once a gene has been identified is to search for homology. Often, gene function can be predicted by looking at homologous genes that have already been assigned a function. There are many model systems that have sequenced genomes and can be examined for proteins similar to the target protein. This method is commonly used when sequencing a new genome because homology can be used to annotate basic and highly conserved genes (Alberts, 2002). However, when the gene is novel and homologues have unknown functions as is the case with CLoG1, other strategies must be used.

Investigating the subcellular localization of the protein may provide insights to its function. For example, a study investigating the localization of a novel Na^+/H^+

exchange protein in yeast uses HA epitope tagging and GFP tagging to create functional fusions that can be assayed for localization. The yeast expressing the HA tagged protein were lysed and separated using a sucrose gradient. The fractions were then assayed with Western blots and SDS-PAGE along with organelle markers to see which organelle the protein would co-fractionate with. In addition, the GFP tagged protein expressing yeast cells were assayed with laser scanning confocal microscopy to visualize the distribution of the protein. Their results showed that the HA-tagged protein co-localized with vacuolar and prevacuolar markers and fractionated away from markers corresponding to the endoplasmic reticulum, plasma membrane and mitochondria. Furthermore, confocal microscopy revealed localization to unique, bipolar perivacuolar compartments (Nass and Rao, 1998).

Another study in yeast looks at novel proteins in the γ -tubulin complex, which is responsible for the organization of microtubules and critical for chromosome segregation and cytokinesis. In order to determine the specific role of these proteins in microtubule function, they were tagged with several different tags including GFP. Along with several deletion assays and protein immunoblotting techniques, the study used microscopy to visualize localization as well as co-localization with known proteins. Their assays show that the proteins of interest localize to spindle pole bodies and the equatorial microtubule-organizing center (EMTOC) (Venkatram et al., 2004).

Project Objectives

The primary goal of this study was to study the intracellular localization and subsequently the function of the CLoG1 protein using *Physcomitrella patens*. After understanding the strategies used in different studies, monomeric enhanced green fluorescent protein (mEGFP) was chosen as a tag for CLoG1. GFP is a protein isolated from a species of jellyfish, which exhibits green fluorescence when exposed to light in the blue to UV range. The aim of the project was to create CLoG1:mEGFP C and N terminal fusions and demonstrate their functional nature using a transient RNAi complementation assay. The goal of this assay was to observe whether the mEGFP tag hindered normal activity of the CLoG1 protein in the fusion by observing growth of the plants.

Once fusions are demonstrated to be functional, the goal was to establish stable lines of wild type (WT) *P. patens* expressing the CLoG1:mEGFP fusions. The fusions are driven by a constitutive promoter, and thus these transformed plants exhibited overexpression of CLoG1, allowing for visualizing the localization of CLoG1 using confocal microscopy. Another aim was to investigate the role of CLoG1 in cell division using a nuclear counting assay. The goal of the assay was to image WT and TS mutant plants expressing nuclearly localized GFP:GUS constructs at different temperatures and count the number of nuclei per plant.

The final goal of the project was to establish several stable lines for future experimentation. The first set is the WT and TS lines expressing an endogenous knock-

in construct containing a mEGFP in frame with the CLoG1 gene. These plants will allow visualization of normal expression levels and patterns of the CLoG1 protein. The second is the TS mutant expressing the CLoG1:mEGFP fusions which can be assayed to see if the wild type CLoG1 can rescue the temperature sensitivity, revealing whether the mutation is a dominant negative or a null mutation. The last line is the WT line expressing the CLoG1:mEGFP fusions along with an mCherry tagged tubulin to observe co-localization.

Methods and Materials

Moss Culture and Protoplasting

The *Physcomitrella patens* moss used was proliferated on PpNH₄ media plates at 25°C with a cycle of 14 hours light and 8 hours dark. Plant tissue from a 7-day-old plate was ground with a homogenizer in 2 mL of dH₂O and 700 µL was transferred onto two PpNH₄ plates overlaid with cellophane. After 7 days, the tissue was collected and incubated for one hour with 3 mL of 2% driselase in 8% mannitol on a shaker in order to remove the cell wall. The resulting protoplasts were then filtered to remove cell debris and centrifuged at 700 rpm for 5 minutes. The pellet was then washed with 8% mannitol two times. The protoplasts were resuspended in 10 mL of 8% mannitol and counted using a hemocytometer.

Transformations

Transformation were performed according to the protocol outlined by Liu (Liu and Vidali, 2011). After pelleting the protoplasts again, the protoplasts were resuspended in enough MMg medium to get a final concentration of 1.6×10^6 protoplasts/mL. After a 20 minute incubation period, 600µL of protoplasts suspension were added to a culture tube with DNA. Transformation were mediated with 700µL of PEG 4000/Ca for 30 minutes. Finally the protoplasts were diluted with 3 mL of W5 and pelleted to remove the PEG, then resuspended in 2 mL of PpNH₄/8% Mannitol/10mM CaCl₂ before being plated in PRMB media with cellophane. The media is a variant of

PpNH₄ containing mannitol to help regulate osmotic pressure of the protoplasts and prevent cell bursting (See Appendix I for media recipes). Four days after transformation the protoplasts were transferred to selective media. For transient transformations, the plants were imaged 7 days after transformation. For stable transformations, the plants were placed onto PpNH₄ after 7 days for one week to promote proliferation and then back onto selection for one week before picking them into a master plate for screening.

CLoG1:mEGFP Fusion Construction

The CLoG1:mEGFP fusion constructs were created using the Invitrogen Multisite Gateway Pro 2.0 kit. For the C-terminal fusions, CLoG1 cDNA was PCR amplified using two primers, attB1CLoG1F and attB5rCLoGR, to produce attB1 and attB5r-flanked CLoG1 cDNA. The primer attB1CLoG1F has the sequence GGG GAC AAG TTT GTA CAA AAA AGC AGG CTT AAT GTC GTT AGC AGA GCA GGA ATC and attB5rCLoGR has the sequence GGG GAC AAC TTT TGT ATA CAA AGT TGT AAG AGT GTT CCC CAT TTC ACT TG. The PCR was done with a 20 µl reaction using New England BioLab (NEB) Inc.'s protocol "PCR Using Q5® High-Fidelity DNA Polymerase (M0491)." The following settings were used according to the NEB's protocol along with their T_m calculator: 98°C for 30 seconds; 30 cycles of: 98°C for 10 seconds, 66°C for 30 seconds, and 72°C for 2 minutes; 72°C for 2 minutes; hold at 4°C. The resulting PCR products were separated on a 0.8% agarose gel and purified using the Machery-Nagel NucleoSpin® Extract II kit.

The flanked PCR fragment was cloned into pDONR P1-P5r vector using a BP reaction according to Invitrogen's Multisite Gateway Pro 2.0 protocol. This entry clone was cloned along with an entry clone containing monomeric enhanced GFP (mEGFP) flanked with attB5 and attB2, into a pTHUbi destination vector using an LR reaction according to the Gateway protocol. The pTHUbi vector contains a hygromycin resistant gene cassette and a maize ubiquitin promoter and allows for efficient targeting to the *P. patens* genomic locus 108.

For the N-terminal fusions, the expression clone was constructed using the same method above however the CLoG1 cDNA PCR fragment was flanked with attB5 and attB2 while the mEGFP was flanked with attB1 and attB5r. The primers used for the CLoG1 cDNA PCR were attB5CLOG1F which has the sequence GGG GAC AAC TTT GTA TAC AAA AGT TGT GTC GTT AGC AGA GCA GGA ATC CTC and attB2CLOG1R which has the sequence GGG GAC CAC TTT GTA CAA GAA AGC TGG GTA TCA AAG AGT GTT CCC CAT TTC AC.

In order to verify the recombination of the fusions, a variety of restriction enzymes were used to digest the entry clones and the fusions. 0.3 µl of the restriction enzymes were added to 0.3 µl of desired clone along with dH₂O, a buffer and BSA. The mixture was incubated for 2 hours at 37°C. The enzyme and clone mixture was then separated on a 0.8% agarose electrophoresis gel. Positive clones, in which the observed band size matched the expected fragment sizes based on the restriction maps of the clones, were sent for direct sequencing using Eton Biosciences. Details of enzyme

combinations and expected fragment sizes can be found Table 1 and restriction gels can be found in Figure 3 in the Results section.

RNAi Complementation Assay

The C and N-terminal fusions were then transiently co-transformed with a 5'UTR RNAi plasmid into the protoplasts of a *P. patens* line called NLS-4 which expresses a nuclearly localized GUS:GFP reporter protein (Vidali et al., 2010). The 5'UTRi construct was made with a 500 bp region of the 5' untranslated region (UTR) of CLoG1. The region was PCR amplified and cloned into a pENTR/D-TOPO plasmid. The plasmid was then inserted into a pUGGi silencing construct using an LR reaction. The pUGGi construct has a loop region flanked by the 5'UTR fragments in opposite orientations, on either side and further flanked by the GUS sequence. The loop region causes the RNA to form a hair pin structure, marking it for cleavage by a dicer. This effectively silences endogenous CLoG1 as well as the nuclear GFP:GUS. The NLS-4 tissue was protoplasted and transformed as described above. There were five transformations conducted: 15 μ g of 5'UTRi; 15 μ g of 5'UTRi with 15 μ g of C-terminus CLoG1:mEGFP; 15 μ g of 5'UTRi with 15 μ g of N-terminus CLoG1:mEGFP; 15 μ g of 5'UTRi with 15 μ g of wild type CLoG1; and 15 μ g of pUGi, a control plasmid which only silences the nuclear GFP:GUS construct. After 7 days, the plants were imaged using a Zeiss Axiovert 200M microscope, with a 10x lens and a long pass emission filter to visualize mEGFP (green) and chlorophyll (red) fluorescence. The images were quantitatively analyzed using an ImageJ macro called

MorphologyMacroVidaliLabV2.8skipTest (see Appendix II). Using the macro, the area and solidity of the plants were measured (Bibeau and Vidali, 2014). Five trials of this assay were conducted. To determine statistical significance, a one-way ANOVA-Tukey was conducted using Origin Pro 8.1. Solidity values were normally distributed however, in order to meet the normality assumption, the areas were log transformed (ln) (Vidali et al., 2007).

Localization

Stables WT lines expressing the CLoG1:mEGFP fusions were established using the transformation protocol described above by Allison Butt, a member of the Vidali lab. Four days after transformation the transformed plants were placed on PpNH₄ with hygromycin plates for one week. They were then transferred to PpNH₄ for one week to allow proliferation and then back on to PpNH₄ with hygromycin for another week. The surviving plants were picked onto a PpNH₄ with hygromycin master plate and successful plants were expanded. Two lines showing low expression of GFP as well as normal morphology were selected and grown on glass bottom MatTek dishes on a thin 70µl layer of agar. These cultures were grown for a week and then tip growing cells were imaged with a Leica SP5 Point Scanning Confocal microscope using the 63X 1.4 NA lens with a hybrid detector. The images of growing cells were acquired at 0.68 second intervals, images of the dividing cells were acquired at 1 second intervals.

Nuclear Counting Assay

Stable lines of WT and TS mutant plants expressing nuclear GFP:GUS were established using the protocol above by Robert Orr, a member of the Vidali lab. Transformed plants were grown at 25°C for four days in a 2mL layer of PRM-T agar and then moved to incubators at different temperatures: 20°C, 25°C and 32°C. Seven days after transformation, plants were stained with calcofluor (cell wall stain) and imaged using a Zeiss Apotome microscope using DAPI and GFP filters and a 10X lens. Maximum intensity projections were created using ImageJ and the macro `enhancemacro` (See Appendix III) was used to threshold particles. Measurements were limited to the threshold and the `analyze particles` function was used to count the number of particles showing an area above 10 pixels. Statistical significance was determined using a one-way ANOVA-Tukey using Origin Pro 8.1.

Results

Restriction Analysis of CLoG1:mEGFP Fusions

In order to investigate the subcellular localization and function of CLoG1, CLoG1 proteins fused with GFP were created. The CLoG1:mEGFP fusions were constructed as outlined by the 'CLoG1:mEGFP fusion construction' section in Methods and Materials. To verify recombination of the constructs, the clones and fusions were digested with restriction enzymes. The combinations of enzymes and clones along with the expected fragment sizes is shown in Table 1.

Table 1. Expected fragment lengths based on restriction maps of clones			
Expected fragment lengths for restriction analysis in Figure 3A			
Lane	Plasmid	Expected length (bp)	Enzymes
1	attL1-CLoG1-attR5 entry clone (undigested)	6428	-
2	attL1-CLoG1-attR5 entry clone	1567, 2130, 2731	XhoI, KpnI, SspI
3	attL5-CLoG1-attL2 entry clone (undigested)	6376	-
4	attL5-CLoG1-attL2 entry clone	1567, 2084, 2725	XhoI, KpnI, SspI
Expected fragment lengths for restriction analysis in Figure 3B			
Lane	Plasmid	Expected length (bp)	Enzymes
1	attL1-meGFP-attR5 entry clone	1015, 2317	EcoRV, AflII
2	attL2-meGFP-attL5 entry clone	966, 2317	EcoRV, AflII
3	CLoG1-5'UTR-RNAi vector	N/A	KpnI, Sac I
4	CLoG1 cDNA control vector	1543, 2999, 3346, 6401	KpnI, NheI
5	CLoG1-meGFP fusion	2290, 2999, 3346, 6401	KpnI, NheI
6	meGFP-CLoG1 fusion	1543, 2999, 4090, 6401	KpnI, NheI

The bands resulting from the restriction analysis, shown in Figure 3, were compared to expected fragment sizes from restriction maps and the comparison revealed successful cloning. For example, attL1 and attR5 flanked CLoG1 entry clone digested with the enzymes XhoI, KpnI, SspI, had expected fragment lengths of 1567, 2130, and 2731 bps. Lane 2 in Figure 3A shows that the observed bands approximately

match these expected lengths. Positive clones identified using this method were then verified by direct sequencing.

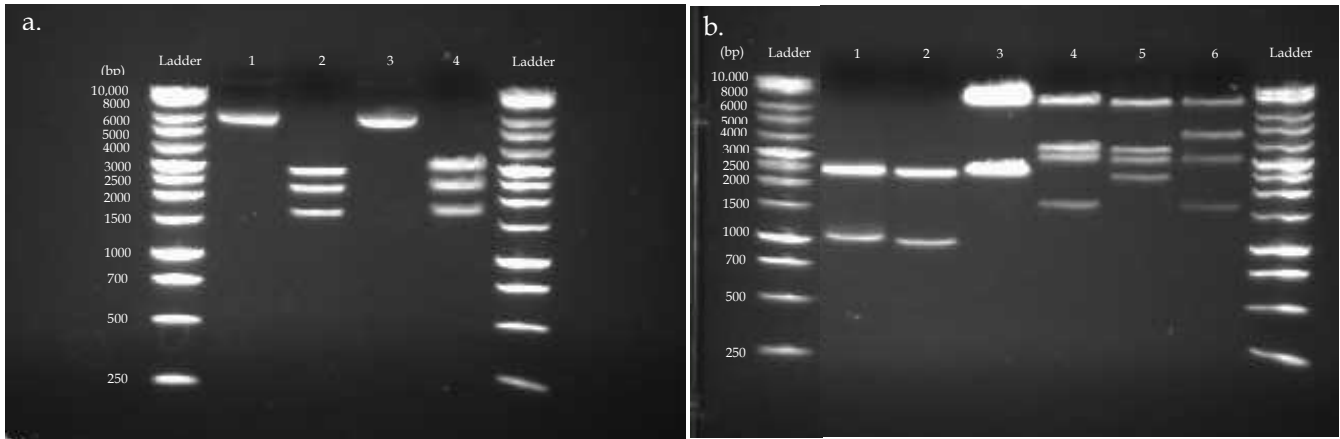


Figure 3. Restriction analysis of (a) CLoG1 entry clones and (b) GFP entry clones, RNAi vector, WT CLoG1 plasmid and CLoG1:mEGFP fusions. Lane contents are described in Table 1.

RNAi Complementation Assay

To evaluate whether the fusions were functional, an RNAi system targeting the 5' UTR of CLoG1 was used along with a complementation assay. RNA interference (RNAi) involves expression of double stranded RNA hairpins targeted for gene silencing. A WT line of *P. patens* expressing a nuclear GFP:GUS construct was co-transformed with RNAi silencing endogenous CLoG1 and CLoG1:mEGFP N or C-terminal fusions. Controls included plants transformed with the RNAi construct only which was the negative control, as well as two positive controls - one co-transformed with RNAi and a CLoG1 cDNA construct and the other transformed with a construct only silencing the nuclear GFP construct. Representative 7 day old transformed plants are shown in Figure 4. The images reveal stunted growth in the negative control, a similar phenotype to TS mutants at the restrictive temperature (Ding, 2014). The CLoG1

cDNA construct seems to fully rescue the RNAi phenotype and both the fusions demonstrate a complete rescue as well.

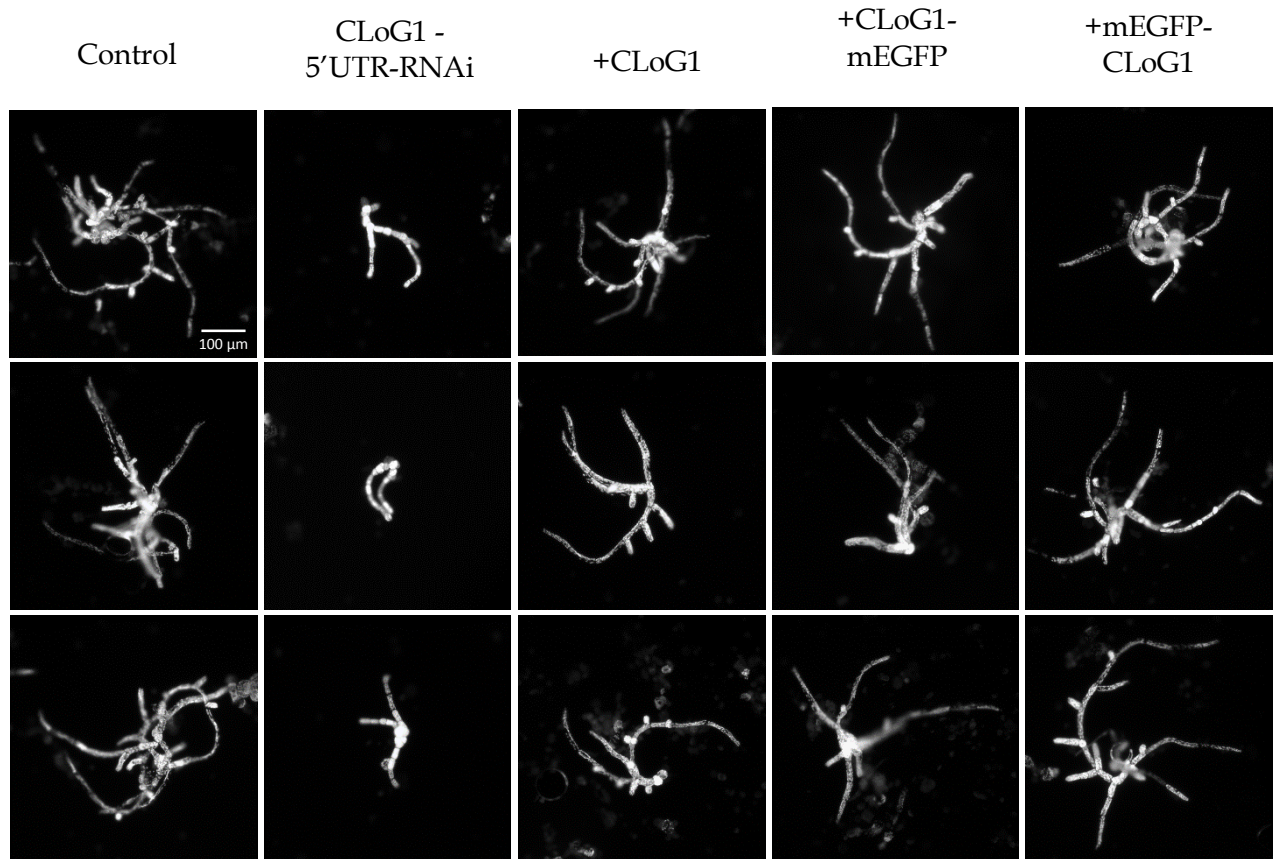


Figure 4. 7-day-old transformed plants expressing a silencing control, only RNAi, RNAi + WT CLoG1, RNAi + CLoG1-mEGFP and lastly mEGFP-CLoG1.

The observed lack of RNAi phenotype in the plants transformed with the fusions is further supported by quantification. Figure 5 shows normalized area and solidity for each condition. The area of the negative control is significantly lower compared to the other four conditions and silenced plant expressing the fusions show no significant difference compared to the positive controls. A similar effect can be seen in the solidity plot. Solidity is the ratio of area to convex hull, thus as branching increases, solidity

decreases. The negative control shows a significantly higher solidity compared to the other four conditions. The C-terminal fusion expressing plants show no significant difference to either of the positive controls while the N-terminal fusion plants cannot be distinguished from the silenced plants expressing the WT CLoG1 plasmids, but are slightly different from the positive silencing control.

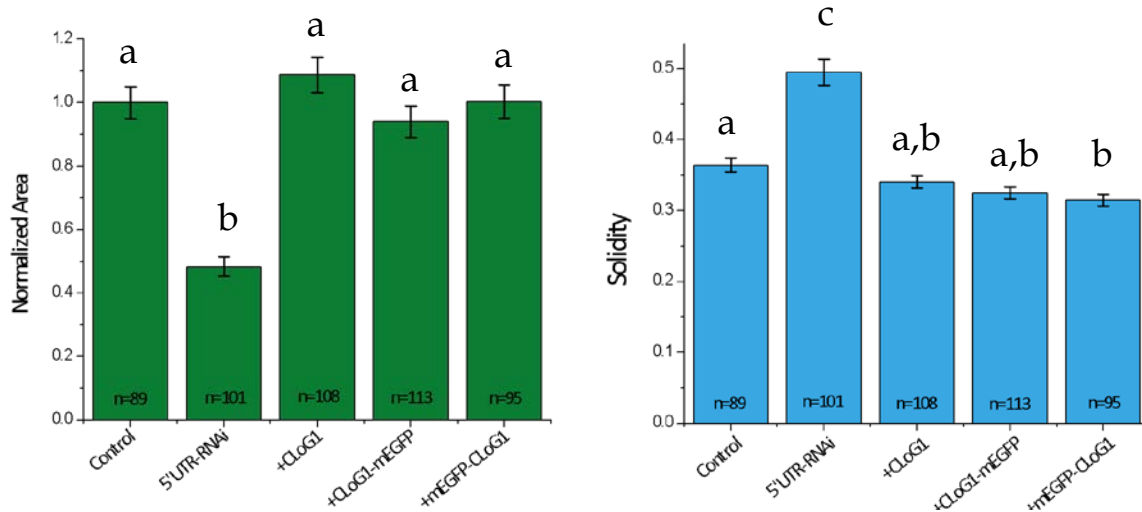


Figure 5. Normalized area and solidity of plants under different condition in the RNAi complementation assay. Letters represent statistical groups that are undistinguishable from each other based on an ANOVA Tukey Test with $p < 0.05$.

Localization

To observe localization of CLoG1, stable lines of WT *P. patens* transformed with CLoG1:mEGFP fusions were established. The stable lines were then cultured on special glass-bottom MatTek plates. Apical cells in the protonemal filaments of the plant were imaged using laser scanning confocal microscopy. Images of plants with the C-terminal fusion are shown in Fig 6a and the N-terminal fusion in Fig 6b. CLoG1 seems to localize

to filamentous structures that appear to be the microtubule cytoskeleton based on size, positioning and dynamics. The filaments are visible in the cell cortex, under the plasma membrane, along with the cytoplasm. The C-terminal fusions seem to have a stronger association to the cortical microtubules while the N-terminal fusions seems to show more intense localization to a spot at the tip of the apical cell. In a cell undergoing division, CLoG1 appears to localize to the mitotic spindle and phragmoplast as shown in Figure 7.

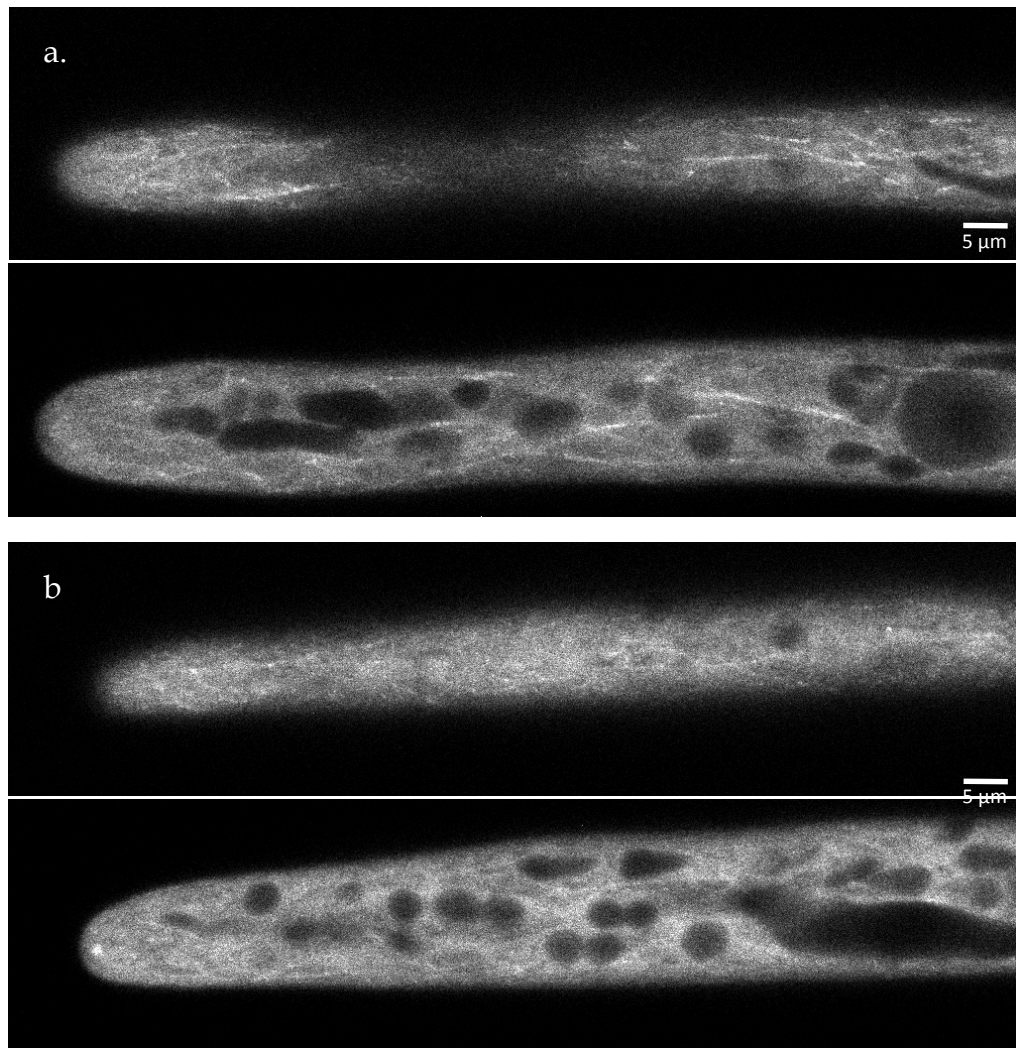


Figure 6. Confocal microscopy of *P. patens* transformed with CLoG1 tagged with GFP showing localization of protein to cortical and cytoplasmic microtubule cytoskeleton.

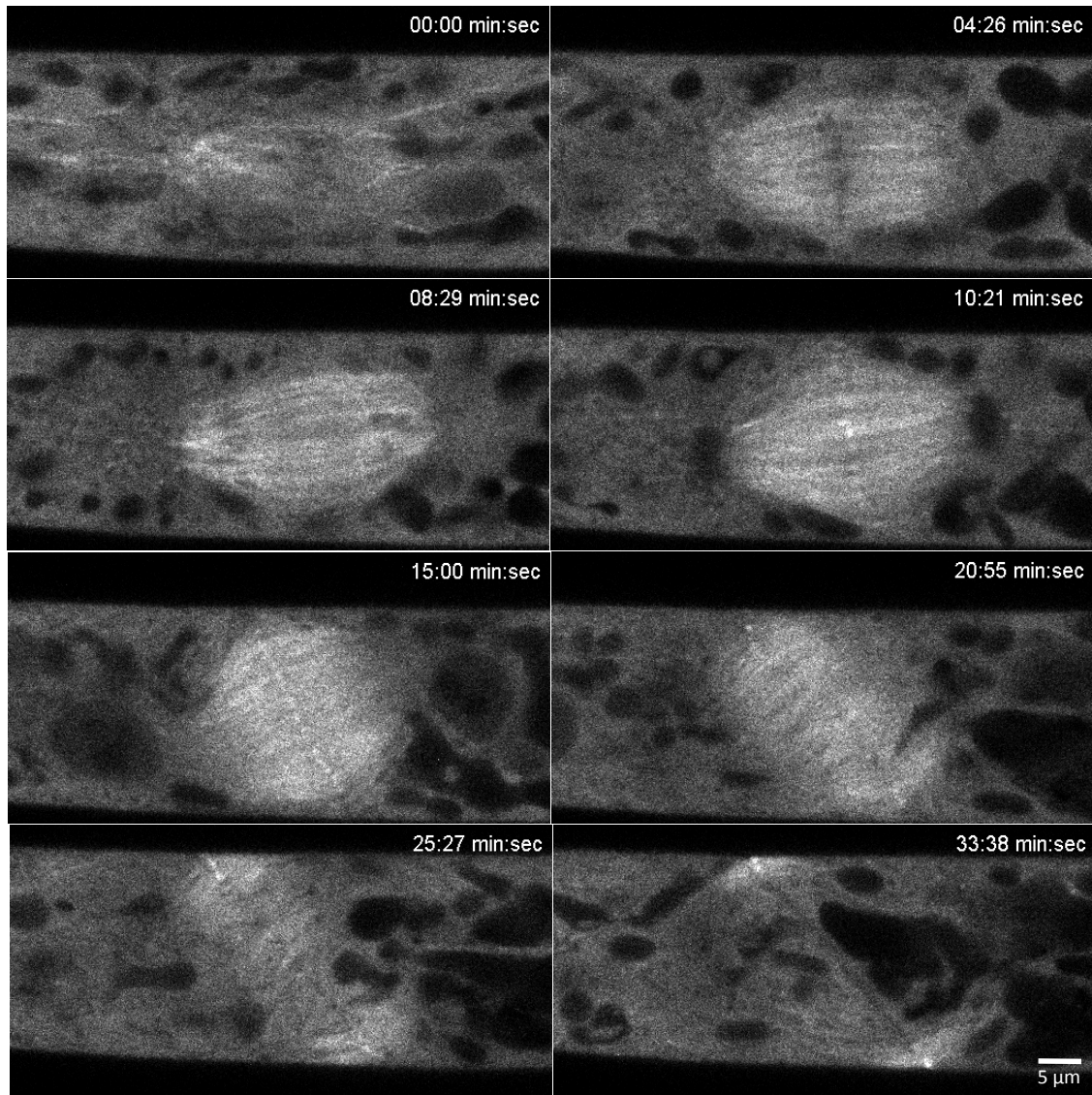


Figure 7. Confocal microscopy of *P. patens* transformed with CLoG1 protein fused with GFP show that CLoG1 localizes to the mitotic spindle and phragmoplast during cell division.

Nuclear Counting Assay

In order to examine the role of CLoG1 in cell division, WT and TS mutant plants expressing nuclear localized GFP:GUS were grown at 20°C, 25°C and 32°C. The plants were stained with calcofluor and imaged as shown in Figure 8. The number of nuclei per plant was counted using an ImageJ macro as outlined in the 'Nuclear Counting Assay' section in Materials and Methods, and the average number of nuclei per plant for each line and temperature is shown in Figure 9. The imaging shows that the growth of the mutants at the restrictive temperature (32°C) is stunted as observed in Ding's study. The imaging also reveals a lack of bi-nucleated or multi-nucleated cells, indicating that the mutant shows no cytokinesis defects. There is no significant difference in the number of nuclei in mutant plants at 32°C compared to 25°C. However, TS mutant plants have significantly fewer nuclei per plant compared to the WT at 32°C, indicating less frequent division events. The WT plants at 25°C also show significantly fewer nuclei per plant compared to the WT at 32°C.

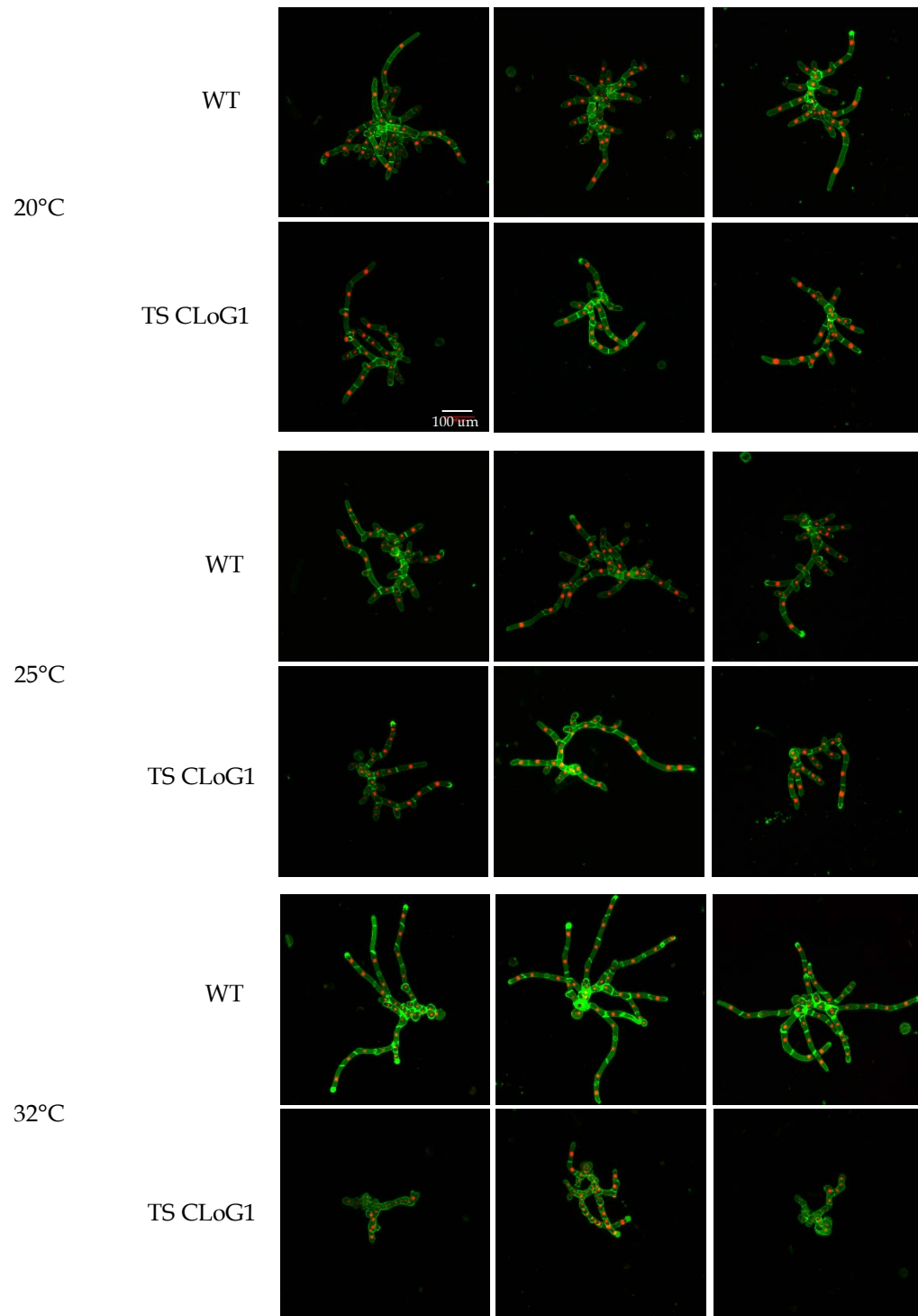


Figure 8. Representative plants of WT and TS mutant plants stained with calcofluor (cell wall stain) grown at different temperatures. The cell wall stain is shown in green and the nuclei in red.

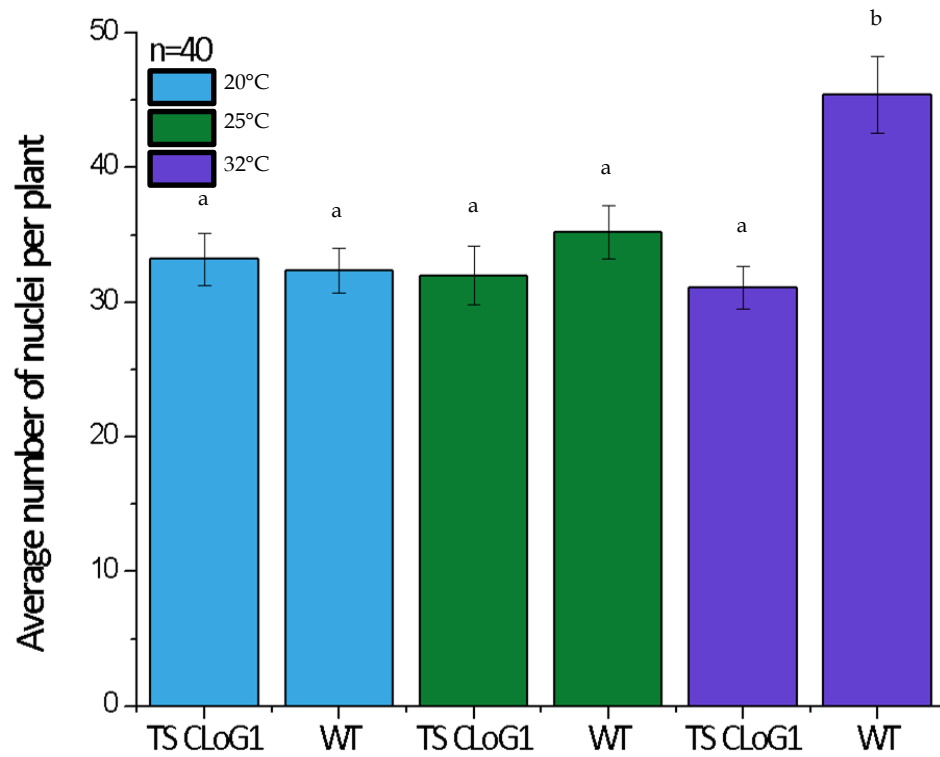


Figure 9. Average number of nuclei per plant for TS and WT lines expressing nuclearly localized GFP grown at different temperatures. Letters represent statistical groups that are undistinguishable from each other based on an ANOVA Tukey Test with $p < 0.05$.

Discussion

With the mutant phenotype characterized and the gene mapped to the *P. patens* genome, the next step for CLoG1 was to investigate the subcellular localization and function of the protein. In this study, CLoG1:mEGFP fusions were created and demonstrated to be functional. They were transformed into WT plants and images using confocal microscopy revealed localization to the microtubule cytoskeleton. The role of CLoG1 in cell division was investigated using a nuclear counting assay, which suggests that CLoG1 caused less frequent cell division in the mutant plants at the restrictive temperature.

Fusion Constructs

Restriction analysis with various enzymes was used to determine if the entry clones and fusions had been correctly constructed. The restriction digests followed by direct sequencing provides irrefutable evidence that the CLoG1 entry clones were constructed correctly. The fusions, following the LR reaction, show evidence of correct recombination based on the restriction analysis however direct sequencing was not conducted. This sequencing step was not necessary because the LR reaction does not involve a PCR step, which can introduce mutation. Furthermore, our positive complementation results, similar to the cDNA construct, suggest that mutations were not present and the protein fusions were constructed correctly. Hence, it is highly unlikely that not sequencing the fusions will cause problems for future

experimentation, however if discrepancies arise in future experiments, it may be advisable to ensure that there are no unexpected base pair substitutions in the regions between the two genes.

RNAi Complementation Assays

An analysis of area and solidity of the plants expressing the controls and the fusions demonstrates that the fusions do not impair growth and thus are functional. It is important to mention that in solidity analysis, the plants transformed with the N-terminal CLoG1:mEGFP fusion are distinguishable from silencing control. However the p value is 0.0229 which is close to the significance level of 0.05. Furthermore, since it is not distinguishable from CLoG1 cDNA control, we can safely assume that N-terminal fusions are functional. Furthermore, the plants transformed with all the CLoG1 constructs show robust cell polarization and elongation. This suggests that even if the N-terminal fusion protein is not fully function, it complements the RNAi phenotype to a large extent, and its localization still provides useful information about CLoG1 function.

Localization

Laser scanning confocal microscopy of apical cells of a *P. patens* WT stable line expressing the CLoG1:mEGFP fusions reveal localization of CLoG1 to the microtubule cytoskeleton in interphase tip growing cells. During cell division, CLoG1 shows localization to the mitotic spindle and the phragmoplast. The N-terminal fusions showed a strong localization to an apical spot in tip growing cell. This spot resembles

the actin spot and myosin which localizes there (Furt et al., 2013). This may suggest that perhaps CLoG1 has transport roles similar to myosin or interacts with microtubules in a similar way to the interaction between myosin and actin. The spot also suggests that microtubules and actin interact in the spot at tip. Similar regions of microtubules and kinesins accumulating at the protonemal apex have been observed (Hiwatashi et al., 2014), suggesting a possible role of CLoG1 in the apical organization of microtubules. The localization to the mitotic spindle supports the observation of microtubule association, since microtubules filaments are central in the formation of mitotic spindle and later the phragmoplast.

Though the localization to the microtubule cytoskeleton is convincing, the expression patterns may be misleading. The fusions constructed for this experiment are driven by a constitutive promoter and thus possibly overexpressed or underexpressed. A possible high expression level may account for the intense localization to the mitotic spindle. With normal expression levels, perhaps CLoG1 will show decreased affinity for the mitotic spindle. Investigation of the endogenous expression patterns is needed to determine if the localization to the mitotic spindle is significant as outlined in the 'Future Experiments' section below.

Nuclear Counting Assay

To explore the role of CLoG1 in cell division, WT and TS mutant plants expressing nuclearly localized GFP were grown at restrictive and permissive temperatures and assayed for number of nuclei per plant. There is a significant difference between the

average number of nuclei per plant in the WT between 25°C and 32°C. This could be due to fact that imaging took place over 8 hours and the samples at 32°C were always taken last, allowing the last plants imaged to divide more than plants at the other two temperatures. Alternatively, perhaps culturing at 32°C causes increased cell division in the WT plants. Ding's data however, does not indicate that the WT line has a higher area at 32°C compared to at 25°C (Ding, 2014). However, the gap between imaging the TS and the mutant at 32°C was short. Thus, the results suggest the TS mutant plants show relative reduction in the average number of nuclei compared to WT plants at 32°C. This indicates that mutation in CLoG1 causes less frequent or slower division. The lack of evidence of bi- or multi-nucleation suggests that there are no problems with cytokinesis completion. Perhaps this means that CLoG1 does not interfere with the mitotic spindle or phragmoplast assembly and instead slows the process down making division occur less frequently in the mutants. If CLoG1 truly plays a role in transport and organization as hypothesized above, the mutant protein may affect the rate at which materials are brought to the cell plate in Golgi-derived vesicles transported along microtubules.

Future Experiments

Clearly, while the intracellular localization of the protein has been made clear, there are many unanswered questions about the function of CLoG1. Future work would include genotyping the CLoG1-mEGFP knock-in *P. patens* lines that were established during the course of this study. These lines can then be used to observe localization

under regular expression levels. Furthermore, the TS mutant lines transformed with the CLoG1:mEGFP fusions need to be assayed to explore if the mutation is dominant. If the fusions can rescue the temperature sensitivity the mutation is null however, if they cannot, the mutation may be dominant. This can provide insight into whether CLoG1 actively plays a role in stunting growth and delaying cell division or if the lack of the functional protein simply affects molecular mechanisms. Lastly, the lines co-expressing tubulin-mCherry and CLoG1:mEGFP should be analyzed to visualize interactions between the microtubule filaments and CLoG1.

References

- Alberts, B.** (2007). *Molecular Biology of the Cell*. New York: Garland Science.
- Bezanilla, M., Perroud, P.F., Pan, A., Klueh, P., and Quatrano, R.S.** (2005). An RNAi system in *Physcomitrella patens* with an internal marker for silencing allows for rapid identification of loss of function phenotypes. *Plant Biol (Stuttg)* **7**, 251-257.
- Bibeau, J.P., and Vidali, L.** (2014). Morphological analysis of cell growth mutants in *Physcomitrella*. *Methods Mol Biol* **1080**, 201-213.
- Borlaug, N.E.** (2000). Ending world hunger. The promise of biotechnology and the threat of antiscience zealotry. *Plant Physiol* **124**, 487-490.
- Burk, D.H., and Ye, Z.H.** (2002). Alteration of oriented deposition of cellulose microfibrils by mutation of a katanin-like microtubule-severing protein. *Plant Cell* **14**, 2145-2160.
- Cove, D.J., Perroud, P.F., Charron, A.J., McDaniel, S.F., Khandelwal, A., and Quatrano, R.S.** (2009). The moss *Physcomitrella patens*: a novel model system for plant development and genomic studies. *Cold Spring Harb Protoc* **2009**, pdb emo115.
- Ding, X.** (2014). Isolation of temperature-sensitive mutants in the moss *Physcomitrella patens* and mapping of their causal mutation by genome sequencing of pooled segregants. BS. Senior Thesis (Major Qualifying Project), Worcester Polytechnic Institute. Advisors: L. Vidali and P. Flaherty

- Furt, F., Liu, Y.C., Bibeau, J.P., Tüzel, E., and Vidali, L.** (2013). Apical myosin XI anticipates F-actin during polarized growth of *Physcomitrella patens* cells. *Plant J* **73**, 417-428.
- Hartwell, L.H.** (1967). Macromolecule synthesis in temperature-sensitive mutants of yeast. *J Bacteriol* **93**, 1662-1670.
- Hepler, P.K., Vidali, L., and Cheung, A.Y.** (2001). Polarized cell growth in higher plants. *Annual Review of Cell and Developmental Biology* **17**, 159-187.
- Hiwatashi, Y., Sato, Y., and Doonan, J.H.** (2014). Kinesins have a dual function in organizing microtubules during both tip growth and cytokinesis in *Physcomitrella patens*. *Plant Cell* **26**, 1256-1266.
- Kost, B., and Chua, N.H.** (2002). The plant cytoskeleton: vacuoles and cell walls make the difference. *Cell* **108**, 9-12.
- Liu, Y.C., and Vidali, L.** (2011). Efficient polyethylene glycol (PEG) mediated transformation of the moss *Physcomitrella patens*. *J Vis Exp* **50**, DOI 10.3791/2560.
- Nass, R., and Rao, R.** (1998). Novel localization of a Na⁺/H⁺ exchanger in a late endosomal compartment of yeast. Implications for vacuole biogenesis. *J Biol Chem* **273**, 21054-21060.
- Nemhauser, J.L., Hong, F., and Chory, J.** (2006). Different plant hormones regulate similar processes through largely nonoverlapping transcriptional responses. *Cell* **126**, 467-475.
- Nishiyama, T., Fujita, T., Shin-I, T., Seki, M., Nishide, H., Uchiyama, I., Kamiya, A., Carninci, P., Hayashizaki, Y., Shinozaki, K., Kohara, Y., and Hasebe, M.** (2003).

- Comparative genomics of *Physcomitrella patens* gametophytic transcriptome and *Arabidopsis thaliana*: Implication for land plant evolution. Proceedings of the National Academy of Sciences of the United States of America **100**, 8007-8012.
- Pervere, L.** (2015). Characterization of conditional loss of growth (CLOg) mutants of *Physcomitrella patens* using proteomics and bioinformatics. BS. Senior Thesis (Major Qualifying Project), Worcester Polytechnic Institute. Advisors: L. Vidali and P. Flaherty
- Prigge, M.J., and Bezanilla, M.** (2010). Evolutionary crossroads in developmental biology: *Physcomitrella patens*. Development **137**, 3535-3543.
- Pringle, J.R.** (1975). Induction, selection, and experimental uses of temperature-sensitive and other conditional mutants of yeast. Methods Cell Biol **12**, 233-272.
- Schaefer, D.G., and Zryd, J.P.** (1997). Efficient gene targeting in the moss *Physcomitrella patens*. Plant Journal **11**, 1195-1206.
- Venkatram, S., Tasto, J.J., Feoktistova, A., Jennings, J.L., Link, A.J., and Gould, K.L.** (2004). Identification and characterization of two novel proteins affecting fission yeast gamma-tubulin complex function. Mol Biol Cell **15**, 2287-2301.
- Vidali, L., McKenna, S.T., and Hepler, P.K.** (2001). Actin polymerization is essential for pollen tube growth. Molecular Biology of the Cell **12**, 2534-2545.
- Vidali, L., Augustine, R.C., Kleinman, K.P., and Bezanilla, M.** (2007). Profilin is essential for tip growth in the moss *Physcomitrella patens*. Plant Cell **19**, 3705-3722.

Vidali, L., Burkart, G.M., Augustine, R.C., Kerdavid, E., Tüzel, E., and Bezanilla, M.

(2010). Myosin XI is essential for tip growth in *Physcomitrella patens*. *Plant Cell* **22**, 1868-1882.

Yuan, J.S., Tiller, K.H., Al-Ahmad, H., Stewart, N.R., and Stewart, C.N., Jr. (2008).

Plants to power: bioenergy to fuel the future. *Trends Plant Sci* **13**, 421-429.

Zhang, H.X., and Blumwald, E. (2001). Transgenic salt-tolerant tomato plants

accumulate salt in foliage but not in fruit. *Nat Biotechnol* **19**, 765-768.

Appendices

APPENDIX I: Moss medium recipes

Moss Medium Recipes		
PpNH ₄	MgSO ₄ · 7H ₂ O - 500X	2 mL
	KH ₂ PO ₄ - 500X	2 mL
	Ca(NO ₃) · 4H ₂ O - 500X	2 mL
	Di-ammonium tartrate	0.5 g
	FeSO ₄ · 7H ₂ O	12.5mg
	Micro elements 1000X	1 mL
	H ₂ O	Up to 1L
	*8g/L of Agar	
PpNO ₃	MgSO ₄ · 7H ₂ O - 500X	2 mL
	KH ₂ PO ₄ - 500X	2 mL
	Ca(NO ₃) · 4H ₂ O - 500X	2 mL
	FeSO ₄ · 7H ₂ O	12.5mg
	Micro elements 100X	1 mL
	H ₂ O	Up to 1L
	*8g/L of Agar	
PRM-B	MgSO ₄ · 7H ₂ O - 500X	2 mL
	KH ₂ PO ₄ - 500X	2 mL
	Ca(NO ₃) · 4H ₂ O - 500X	2 mL
	Di-ammonium tartrate	2 mL (or 0.5 g)
	FeSO ₄ · 7H ₂ O	12.5mg
	Micro elements 1000X	1 mL
	Mannitol	60g
	H ₂ O	Up to 1L
	*10mL of 1M CaCl ₂ stock after autoclaving	
	*8g/L of Agar	
PRM-T	MgSO ₄ · 7H ₂ O - 500X	2 mL
	KH ₂ PO ₄ - 500X	2 mL
	Ca(NO ₃) · 4H ₂ O - 500X	2 mL
	Di-ammonium tartrate - 500X	2 mL
	FeSO ₄ · 7H ₂ O	12.5mg (must weigh this out, don't prepare stock)
	Micro elements 1000X	1 mL
	Mannitol	60g
	H ₂ O	Up to 1L
	*10mL of 1M CaCl ₂ stock after autoclaving	
	*4g/L of Agar	
PpNH ₄ and hygromycin	Prepare PpNH ₄ according to recipe above. Add 300ul of 50mg/ml of hygromycin stock to 1L of medium after autoclaving.	

MMg Buffer	For 100 mL:		
		Stock	Final Concentration
			Final Volume
	Mannitol	0.8 M	0.4 M
	MgCl ₂	150 mM	15 mM
	MES	20 mM pH 5.7	4 mM
W5 Buffer	H ₂ O		20 mL
	For 100 mL:		
		Stock	Final Concentration
			Final Volume
	NaCl	500 mM	154 mM
	CaCl ₂	1M	125 mM
	KCl	50 mM	5 mM
	MES	20 mM pH 5.7	2 mM
	H ₂ O		36.7 mL

APPENDIX II: ImageJ macro for area and solidity quantification created by Jeffrey Bibeau, a member of the Vidali Lab

```
//My version of the shaving macro that does not require
//installation or pressing numbers
//It also doesn't matter how many channels you have
```

```
requires("1.47d");
```

```
//This section comes from the macro: Zeiss-RGB-red-green-merger.txt
//Takes tiff images from the zeiss discovery microscope and makes color stacks (RGBs optional)
```

```
//Lets the user name their file
Dialog.create("Name");
default="Blank";
Dialog.addMessage("What is the name? ");
Dialog.addString("yymmddconstruct", default);
Dialog.show();
original=Dialog.getString();
```

```
rename(original);
```

```
setSlice(1);
```

```

selectWindow(original);
rename("red");
//run("Duplicate...", "title=green duplicate range=1-any");

//selectWindow("red");
//nnew=nSlices/3;

//for (k=1; k<=nnew; k++) {
    //setSlice(k+1);
    //run("Delete Slice");
    //setSlice(k+1);
    //run("Delete Slice");
//}

//selectWindow("green");
//setSlice(1);
//nnew=nSlices/3;
//run("Delete Slice");

//for (k=1; k<nnew; k++) {
    //setSlice(k+1);
    //run("Delete Slice");
    //setSlice(k+1);
    //run("Delete Slice");
//}
//setSlice(nnew+1);
//run("Delete Slice");

//run("Merge Channels...", "red=red green=green blue=*None* gray=*None* create");

//run("RGB Color", "slices");

rename(original);

//Lets the user set the scale of the image
Dialog.create("Scale");
default=1;
Dialog.addMessage("What is the image scale in pixels per micrometer?") ;
Dialog.addNumber("pixels/um", default) ;
Dialog.show();
pixelum=Dialog.getNumber();

```

```

// Lets the user set the pixel saturation for enhancement
Dialog.create("Pixel Saturation");
default=0;
Dialog.addMessage("Input pixel saturation between 0 and 1 for image enhancement");
Dialog.addNumber("Pixel Saturation", default);
Dialog.show();
pixsat=Dialog.getNumber();

// Renames the current image stack
setSlice(1);
original = getTitle();
selectWindow(original);

// This determines how to interpret the image
// It figures out how many channels the image has
getDimensions(widthpix, heightpix, channels, slices, frame);

rows = 2;
columns = 1;
color = newArray(rows);
default = newArray(rows);
color[0] = "Color";
color[1] = "Black and White";

for (i=0; i<rows; i++) {
    if ((i%2)==0)
        default[i] = true;
    else
        default[i] = false;
}
ans=newArray(rows);
Dialog.create("Color or Black and White");
Dialog.addMessage("Are your images Color or Black and White?");
Dialog.addCheckboxGroup(rows,columns,color,default);
Dialog.show();
for (i=0; i<rows; i++)
{
color[i]=Dialog.getCheckbox();
}

getDimensions(widthpix, heightpix, channels, slices, frame);

```

```

if(color[0]==1&&channels==1)
{
run("RGB Stack");
}
else
{
run("16-bit");
run("Enhance Contrast...", "saturated=pixsat normalize process_all");
}

//This allows for the user to see the contrast enhancement
if(color[0]==1&&channels==3)
{
run("RGB Split");
selectImage(3);
rename("blue");
selectImage(2);
rename("green");
run("Enhance Contrast...", "saturated=pixsat normalize process_all");
selectImage(1);
rename("red");
run("Enhance Contrast...", "saturated=pixsat normalize process_all");
run("Merge Channels...", "red=red green=green blue=blue gray=*None* create");
rename(original);
}

if(color[0]==1&&channels==2)
{
run("RGB Split");
selectImage(2);
rename("green");
run("Enhance Contrast...", "saturated=pixsat normalize process_all");
selectImage(1);
rename("red");
run("Enhance Contrast...", "saturated=pixsat normalize process_all");
run("Merge Channels...", "red=red green=green blue=*None* gray=*None* create");
rename(original);
}

getDimensions(widthpix, heightpix, channels, slices, frame);

//First portion of this array is the channel(red is 1 green is 2)

```



```

//Second position is the slice

Stack.setPosition(1,1,1);
var original = "a string";
var dest = "a string";

original = getTitle();
destshave = original+"shaved";
//frames is the number of slices in the image
frames = slices;

//keeps RGBs RGBs
if(color[0]==1)
{
newImage(destshave, "RGB black", widthpix, heightpix, frames);
}

//Keeps black and white 16-bit
if(color[1]==1)
{
newImage(destshave, "16-bit black", widthpix, heightpix, frames);
}

////////////////////////////////////
///
//////////While loop that makes sure you are on a frame less than the last
//Runs the copy and paste so that your shaved images go into the proper
//stack////////////////////////////////////
//
Stack.getPosition(ch,sl,fr);
while(sl<frames)
{
selectWindow(original);

setTool(3);

if(sl>1)
{run("Restore Selection");};

waitForUser("Selection","Finish shaving and press OK to continue. Skip frames when
necessary");
if(sl<frames)
{

```

```

selectWindow(original);
run("Copy");
selectWindow(destshave);
run("Paste");
nextshave=getSliceNumber+1;
setSlice(nextshave);
selectWindow(original);
Stack.getPosition(c,s,f);
nextoriginal=s+1;
sl=nextoriginal;
Stack.setPosition(1,nextoriginal,1);
}
}

```

```

selectWindow(original);

```

```

////////////////////////////////////
///

```

```

//if statement that checks if the frame you are on is the last one////////

```

```

//User can decide to shave or skip

```

```

it////////////////////////////////

```

```

Stack.getPosition(c,sl,f);

```

```

if(sl==frames)

```

```

{

```

```

label=newArray("yes");

```

```

default=newArray("1");

```

```

Dialog.create("Last Image");

```

```

Dialog.addMessage("Do you want to shave the last image");

```

```

Dialog.addCheckboxGroup(1,1,label,default);

```

```

Dialog.show();

```

```

answer=newArray(1);

```

```

for (i=0; i<1; i++)

```

```

{answer[i]=Dialog.getCheckbox();}

```

```

if(answer[0]==1)

```

```

{

```

```

run("Restore Selection");

```

```

waitForUser("Selection","Finish shaving and press OK to continue.");

```

```

selectWindow(original);

```

```

run("Copy");

```

```

selectWindow(destshave);

```

```

run("Paste");

```

```

last=0;
}
if(answer[0]==0)
{last=1;}
}

////////////////////////////////////
////
//Portion in which the program truncates the blank stacks in dest////////
////////////////////////////////////
///
selectWindow(original);
close;

requires("1.38m");
setBatchMode(true);

selectWindow(destshave);

subtract=frames-getSliceNumber+last;

if(subtract>0){
for (i=0; i<subtract; i++)
{
setSlice(frames-i);
run("Delete Slice");
}
}
////////////////////////////////////
////
requires("1.38m");
setBatchMode(true);

//Gets the title of your current window
selectWindow(destshave);

name = getTitle();

//Creates more strings from name of destshave
DatePlated = substring(name, 0, 6);
constuctnamelength=lengthOf(name)-6;
Construct = substring(name, 6, constuctnamelength);
Constructlenght=lengthOf(Construct)-4;

```

```

newConstruct=original;
//newConstruct=substring(Construct,0,Constructlength);
Color = substring(name, constuctnamelength, lengthOf(name));

if(color[0]==1)
{
//Splits the RGB into 3 channels and then deletes the extraneous channels
run("RGB Split");
selectImage(3);
close;
selectImage(2);
close;
selectImage(1);
}

//Gets the title and calls it test?
var test = getTitle();

//Selects the window you just calles test
selectWindow(test);

//Sets the slice of test to 1
setSlice(1);

run("Set Scale...", "distance=1 known=1 pixel=1 unit=um global");

//Initializes a bunch of arrays that should measure the the characteristics of the image
c=0;
PreResLabel=newArray(nSlices);
PreResArea=newArray(nSlices);
PreResPer=newArray(nSlices);
PreResCHA=newArray(nSlices);
PreResPE=newArray(nSlices);
PreResSol=newArray(nSlices);
PreResCo=newArray(nSlices);
PreResCi=newArray(nSlices);
LowerThreshold= newArray(nSlices);

for(k=1; k<=nSlices; k++) {

//Refer to notes on Otsu and Max entropy thresholding but essentially assumes
//bimodal distribution, the point of separation of the two distributions is set

```

```

//by finding the point that reduces the uncertainty in the two histograms
//porbability distribution

//sets the threshold to max entropy changing the image to a binary
setAutoThreshold("MaxEntropy dark");

//gets the value of that threshold, where it stores the value of the threshold into
an array
getThreshold(LowerThreshold[k-1], UpperThreshold );

//Sets the measurement tool to the listed properties
run("Set Measurements...", "area perimeter circularity limit display decimal=4 ");

//Runs a command that has the ability to analyze a thresholded image
run("Analyze Particles...", "size=0-Infinity circularity=0.00-1.00 show=Nothing
display clear record slice");

//Determines if there are more than one thresholded complete images
n = nResults;

    if (nResults>1){

//If statement that produces an array called area1a which records the image statistics
for each results

        area1a = newArray(n);
        length1a = newArray(n);

        circularity1a = newArray(n);
        label1a = newArray(n);

        xstarta = newArray(n);
        ystarta = newArray(n);

//For loop that determines the result with the highest area and stores that result as
NewArea
        for (i=0; i<nResults; i++)

            area1a[i] = getResult('Area', i);

newArea = 0;
totalArea = 0;
for (i=0; i<nResults; i++) {

```

```

totalArea = totalArea + area1a[i];
if (area1a[i]>newArea) {
index = i;
newArea = area1a[i];
}

}

label1 = getResultLabel(index);

area1 = getResult('Area', index);

area3 = totalArea;
length1 = getResult('Perim.', index);
circularity1 = getResult('Circ.', index);

xstart = getResult('XStart', index);
ystart = getResult('YStart', index);

}

//Else statment that is conducted if there is only one area result
else{

for (i=0; i<n; i++) {
label1 = getResultLabel(i);
area1 = getResult('Area', i);

area3 = getResult('Area', i);
length1 = getResult('Perim.', i);
circularity1 = getResult('Circ.', i);

xstart = getResult('XStart', i);
ystart = getResult('YStart', i);}}

run("Clear Results");
for (i=0; i<1; i++) {
doWand(xstart, ystart);
run("Convex Hull");
run("Set Measurements...", "area perimeter");
run("Measure");

```

```

    area2 = getResult('Area', i);
    length2 = getResult('Perim.', i);
}

//Makes sure nothign is selected
run("Select None");

    PreResLabel[c]= label1;

    PreResArea[c]=area3;
    PreResPer[c]= length1;
    PreResCHA[c]=area2;
    PreResPE[c]=length2;
    PreResSol[c]=area1/area2;
    PreResCo[c]=length2/length1;
    PreResCi[c]=circularity1;

c=c+1;
//Goes to the next slice of the stack
run("Next Slice [>]");
}

sort(PreResArea);

function sort(PreResArea) {quickSort(PreResArea, PreResLabel, 0,
lengthOf(PreResArea)-1);}

function quickSort(PreResArea, PreResLabel, from, to) {
    i = from; j = to;
    center = PreResArea[(from+to)/2];
    do {
        while (i<to && center>PreResArea[i]) i++;
        while (j>from && center<PreResArea[j]) j--;
        if (i<j) { tempA=PreResArea[i];
            tempL= PreResLabel[i];
            PreResArea[i]=PreResArea[j];
            PreResLabel[i]=PreResLabel[j];
            PreResArea[j]=tempA;
            PreResLabel[j]=tempL;}
        if (i<=j) {i++; j--;}
    } while(i<=j);
    if (from<j) quickSort(PreResArea, PreResLabel, from, j);
    if (i<to) quickSort(PreResArea, PreResLabel, i, to);
}

```

```

}

function list(PreResArea) {
    for (i=0; i<c; i++)
        print(PreResLabel[i], ", ", PreResArea[i]);
    print("");
}

SizedArray = newArray(nSlices);
for (i=0; i<nSlices; i++) {
    dospuntos = lastIndexOf(PreResLabel[i], ":");
    SizedArray[i] = substring(PreResLabel[i], dospuntos+1, lengthOf(PreResLabel[i]));
}

title1 = "PhenotypeResults";
title2 = "["+title1+"]";
f = title2;
if (isOpen(title1))
    print(f, "\\Clear");
else
    run("New... ", "name="+title2+" type=Table width=250 height=600");
print(f,
"\\Headings:Date\\tConstruct\\tIndex\\tArea(um^2)\\tCircularity\\tSolidity\\tThreshold\\tPerimeter(um)\\tConvexity\\tCHArea(um^2)\\tCHPerim(um)");
for (i=0; i<c; i++) {

    print(f, DatePlated + "\\t" + Construct + "\\t"+SizedArray[i]+"\\t"+
PreResArea[i]/(pow(pixelum,2)) + "\\t" + PreResCi[i]+ "\\t" + PreResSol[i]+ "\\t" +
LowerThreshold[i]+ "\\t" + PreResPer[i]/(pixelum)+ "\\t" + PreResCo[i]+ "\\t" +
PreResCHA[i]/(pow(pixelum,2))+ "\\t" + PreResPE[i]/(pixelum));

}

selectImage(1);
original = getTitle();
dest = original+"sized"+"tif";
binary=original+"binary"+"tif";
frames = nSlices;
newImage(dest, "8-bit black", widthpix, heightpix, frames);
newImage(binary, "8-bit black", widthpix, heightpix, frames);
newImage("temp", "8-bit black", widthpix, heightpix, 1);

```



```

//For loop that copies each slice of the original image and pastes them into the new
sorted and resized image
// Instead of selecting original here we might want to select the binary image
for (i=0; i<nSlices;i++) {

SliceActive=SizedArray[i];
// Here is where I am going to add a new image stack that will be a binary image
// This make the binary image and then sorts it just like the other images

selectWindow(original);
setSlice(SliceActive);
run("Copy");

selectWindow(dest);
setMetadata(PreResLabel[i]);
run("Paste");
run("Next Slice [>]");

selectWindow("temp");
run("Paste");

setAutoThreshold("MaxEntropy dark");
getThreshold(Lower,Upper);
// print(Lower);
// print(Upper);
run("Make Binary", "thresholded remaining black");
run("Copy");

selectWindow(binary);
setSlice(i+1);
setMetadata(PreResLabel[i]);
run("Paste");
run("Next Slice [>]");
}

selectWindow("temp");
close;

//Quick macro I wrote with the capacity to create multiple montages
//This macro also takes the binary window and makes a montage from it
//It would be easy to make this also produce a non binary montage

selectWindow(binary);

```

```

run("Enhance Contrast...", "saturated=0 normalize process_all");
windows=(floor((nSlices()/50)))+1;

for(i=1; i<=windows; i++)
{

selectWindow(binary);
setForegroundColor (0, 0, 0);

setBackgroundColors(255, 255, 255);

//Specifies which frames the montage will start and end with
firstframe=((i*50)+1)-50;
lastframe=((i*50)+1);

run("Make Montage...", "columns=5 rows=10 scale=.25 first=firstframe last=lastframe
increment=1 border=1 label use");
//run("Invert");
setBackgroundColors(255,255,255);
getMinAndMax(min, max);
setColor(min);

setFont("SansSerif", 40);
getDimensions(width, height, channels, slices, frames);
setJustification("center");

drawString(binary, width/2, 50);

//enables the user to determine the order of their newly formed windows
selectWindow("Montage");
rename("Binary"+i);

//This makes a montage of the non-binary image
selectWindow(dest);
run("Enhance Contrast...", "saturated=0 normalize process_all");

setForegroundColor (255, 255, 255);
setBackgroundColors(0, 0, 0);
run("Make Montage...", "columns=5 rows=10 scale=.25 first=firstframe last=lastframe
increment=1 border=1 label use");
run("Invert");
setBackgroundColors(255,255,255);
getMinAndMax(min, max);

```

```

setColor(min);
setFont("SansSerif", 40);
getDimensions(width, height, channels, slices, frames);
setJustification("center");
drawString(binary, width/2, 50);
rename("NonBinary"+i);
}

if(windows>1)
{
run("Images to Stack", "name=NormalMontage title=[NonBinary] use");
}
else
{
selectWindow("NonBinary1");
rename("NormalMontage");
}

if(windows>1)
{
run("Images to Stack", "name=Montage title=[Binary] use");
}
else
{
selectWindow("Binary1");
rename("Montage");
}

rows = 5;
columns = 1;
labels = newArray(rows);
defaults = newArray(rows);
labels[0] = "Binary Montage";
labels[1] = "Montage";
labels[2] = "Phenotype Results Table";
labels[3] = "Sorted Image Stack";
labels[4] = "Sorted Binary Image Stack";

for (i=0; i<rows; i++) {

if ((i%2)==0)
    defaults[i] = true;
else

```

```

        defaults[i] = false;
    }
    answers=newArray(rows);
    Dialog.create("What files would you like to save?");
    Dialog.addMessage("Select the files you would like to save");
    Dialog.addCheckboxGroup(rows,columns,labels,defaults);
    Dialog.show();
    for (i=0; i<rows; i++)
    {
        answers[i]=Dialog.getCheckbox();
    }

    if(answers[0]==0 && answers[1]==0 && answers[2]==0 && answers[3]==0 &&
    answers[4]==0)
    {run("Close All");
    setBatchMode(false);
    waitForUser("Macro is completed");
    }

    else
    {

        //This asks the user if they want to save their files in the same place
        label=newArray("yes");
        default=newArray("1");
        Dialog.create("Save files in one place?");
        Dialog.addMessage("Save files in one place?");
        Dialog.addCheckboxGroup(1,1,label,default);
        Dialog.show();

        answer=newArray(1);
        for (i=0; i<1; i++)
        {
            answer[i]=Dialog.getCheckbox();
        }

        if(answer[0]==1)
        {
            //This will let people save their file

            waitForUser("Selection","Press OK to continue to the file path where you would like to
            save files");

```

```

dir=getDirectory("Choose your directory");

// Binary Montage
if(answers[0]==1)
{selectWindow("Montage");
saveAs(".tif", dir+newConstruct+"BinaryMontage"+".tif");
}

// Normal Montage
if(answers[1]==1)
{selectWindow("NormalMontage");
saveAs(".tif", dir+newConstruct+"Montage"+".tif");
}

// Results Table
if(answers[2]==1)
{
selectWindow(title1);
saveAs("Text", dir+newConstruct+"PhenotypeResults"+".txt");
}

// Sorted Image Stack
if(answers[3]==1)
{selectWindow(dest);
saveAs(".tif", dir+newConstruct+"SortedStack.tif");
}

// Sorted Binary Image Stack
if(answers[4]==1)
{selectWindow(binary);
saveAs(".tif", dir+newConstruct+"BinarySortedStack.tif");
}

}

else
{
// Binary Montage
if(answers[0]==1)
{
waitForUser("Selection","Press OK to find the file path for the binary montage");

dir=getDirectory("Choose your directory");

```

```

selectWindow("Montage");
saveAs(".tif", dir+newConstruct+"BinaryMontage"+" .tif");
}

//Normal Montage
if(answers[1]==1)
{
waitForUser("Selection","Press OK to find the file path for the normal montage");

dir=getDirectory("Choose your directory");

selectWindow("NormalMontage");
saveAs(".tif", dir+newConstruct+"Montage"+" .tif");
}

//Results Table
if(answers[2]==1)
{
waitForUser("Selection","Press OK to find the file path for your results table");

dir=getDirectory("Choose your directory");

selectWindow(title1);
saveAs("Text", dir+newConstruct+"PhenotypeResults"+" .txt");
}

//Sorted Image Stack
if(answers[3]==1)
{waitForUser("Selection","Press OK to find the file path for your sorted image stack");

dir=getDirectory("Choose your directory");

selectWindow(dest);
saveAs("Tif", dir+newConstruct+"SortedStack.tif");
}

//Sorted Binary Image Stack
if(answers[4]==1)
{waitForUser("Selection","Press OK to find the file path for your sorted image stack");

dir=getDirectory("Choose your directory");

```

```

selectWindow(binary);
saveAs("Tif", dir+newConstruct+"BinarySortedStack.tif");
}

}

selectImage(1);
close;
selectImage(1);
close;
selectImage(1);
close;
selectImage(1);
close;
selectImage(1);
close;
selectImage(1);
close;

setBatchMode(false);

waitForUser("Macro is completed");
}

```

APPENDIX III: ImageJ macro for nuclear counting

```

run("Duplicate...", "duplicate channels=1");

run("Grays");

setAutoThreshold("IsoData dark");

//run("Threshold...");

```